

Article

Not peer-reviewed version

---

# Synthesis and Characterization of TiO<sub>2</sub> Nanotubes for High-Performance Gas Sensor Application

---

[Belgacem Bouktif](#)<sup>\*</sup>, Anouar Hajjaji, [Karim Choubani](#), [Nashmi H. Alrasheedi](#), Wissem Dimassi, [Mohamed Ben Rabha](#)<sup>\*</sup>

Posted Date: 25 October 2024

doi: 10.20944/preprints202410.1915.v1

Keywords: Metal Oxides; Crystal Structure; Titanium dioxide; Electrochemical; Nanotubes; Gas sensors



Preprints.org is a free multidisciplinary platform providing preprint service that is dedicated to making early versions of research outputs permanently available and citable. Preprints posted at Preprints.org appear in Web of Science, Crossref, Google Scholar, Scilit, Europe PMC.

Copyright: This open access article is published under a Creative Commons CC BY 4.0 license, which permit the free download, distribution, and reuse, provided that the author and preprint are cited in any reuse.

## Article

# Synthesis and Characterization of TiO<sub>2</sub> Nanotubes for High-Performance Gas Sensor Applications

Belgacem Bouktif <sup>1,\*</sup>, Anouar Hajjaji <sup>2</sup>, Karim Choubani <sup>3</sup>, Nashmi H. Alrasheedi <sup>3</sup>,  
Wissem Dimassi <sup>4</sup> and Mohamed Ben Rabha<sup>4,\*</sup>

<sup>1</sup> University Sains Malaysia 11800 Gelugor, Penang, Malaysia

<sup>2</sup> LPV, Centre de Recherches et des Technologies de l'Énergie, Technopôle de Borj-Cédria, BP 95 Hammam-Lif, Tunis, 2050, Tunisie

<sup>3</sup> Department of Mechanical Engineering, College of Engineering, Imam Mohammad Ibn Saud Islamic University, Riyadh, Saudi Arabia

<sup>4</sup> LANSER, Centre de Recherches et des Technologies de l'Énergie, Technopôle de Borj-Cédria, BP 95 Hammam-Lif, Tunis, 2050, Tunisie

\* Correspondence: belgacem.bouktif@gmail.com (B.B.); rabha2222@yahoo.fr (M.B.R.)

**Abstract:** In this present work, we investigated the fabrication, properties, and sensing applications of TiO<sub>2</sub> nanotubes. A pure titanium metal sheet was used to demonstrate how titanium dioxide nanotubes can be used for gas-sensing applications through the electrochemical anodization method. Subsequently, X-ray diffraction indicated the crystallization of the titanium dioxide layer. Scanning electron microscopy and transmission electron microscopy then revealed the average diameter of the TiO<sub>2</sub> nanotubes to be approximately 100 nm, with tube lengths ranging between 3 and 9 μm and the thickness of the nanotube walls being about 25 nm. This type of TiO<sub>2</sub> nanotube was found to be suitable for NO<sub>2</sub> gas sensor applications. With an oxidation time of 15 min, its detection of NO<sub>2</sub> gas showed good result at 250 °C, especially when exposed to a NO<sub>2</sub> gas flow of 100 ppm, where a maximum NO<sub>2</sub> gas response of 96% was obtained. The NO<sub>2</sub> sensors based on the TiO<sub>2</sub> nanotube arrays all exhibited a high level of stability, good reproducibility, and high sensitivity.

**Keywords:** titanium dioxide; electrochemical anodization; TiO<sub>2</sub> nanotubes; gas sensors

## 1. Introduction

In recent years, significant attention has focused on advancing NO<sub>2</sub> sensors by employing metal oxide semiconductors, such as SnO<sub>2</sub>, In<sub>2</sub>O<sub>3</sub>, ZnO, and WO<sub>3</sub>, [1–4]. TiO<sub>2</sub> nanotube arrays [5,6], however, offer several distinct advantages over these materials for NO<sub>2</sub> sensing beyond their large surface-to-volume ratio. Indeed, TiO<sub>2</sub> nanotubes have tunable physical and electronic properties [7,8] that allow for more precise control over a sensor's sensitivity through modifications in the TiO<sub>2</sub> nanotubes' crystallinity, diameter, length, and wall thickness. Furthermore, TiO<sub>2</sub> nanotubes show excellent electron mobility, which can improve sensor response times and overall sensitivity when compared to other metal oxides. Such properties make TiO<sub>2</sub> nanotubes very promising for various applications in a number of fields. They also have enormous potential for development compared with other nanostructure forms in fields like photocatalysis [8] and energy storage [9]. Moreover, TiO<sub>2</sub> nanotubes exhibit outstanding sensitivity and selectivity for many distinct gases, including H<sub>2</sub> [10,11], NO<sub>2</sub> [12], NO<sub>x</sub> [13], CO [14], NH<sub>3</sub> [15], and H<sub>2</sub>S [16,17], as well as Volatile Organic Compounds (VOCs). Various techniques have been applied to fabricate TiO<sub>2</sub> nanotubes [18], such as electrochemical anodization [19–21]. The production of TiO<sub>2</sub> nanotubes on a titanium sheet through anodization is the best process for yielding highly ordered and organized nanostructures. Toxic gases like CO, SO<sub>2</sub>, H<sub>2</sub>S, NO<sub>x</sub>, and so on are harmful to human life and the environment, so there is a need for gas detectors to detect and subsequently control leaks of these unsafe gases. Extending the lifetime of sensors based on TiO<sub>2</sub> also provides more opportunities for developing new high-quality sensors.

To expand the use of titania nanostructures in fabricating gas sensors, some physical parameters need to be improved, namely the sensing signal, the response, and the recovery times. Several nanostructures have been used to fabricate gas detectors, one of them being vertical  $\text{TiO}_2$  nanotube arrays prepared using electrochemical anodization, which have numerous oxygen vacancies that provide effective gas diffusion and more active sites. They are considered an ideal platform for gas sensing due to their fast response, high sensitivity, low cost, and long-term stability [22].

In this present study, a  $\text{TiO}_2$  nanotube array was used for  $\text{NO}_2$  gas sensing. A simple electrochemical anodization on a titanium sheet yielded layers of self-organized  $\text{TiO}_2$  nanotubes. X-ray diffraction (XRD) and other analytical methods were then used to characterize the properties of the nanomaterials. The morphology and microstructure of these layers were then determined using a scanning electron microscope (SEM) and transmission electron microscope (TEM), respectively.

Outdoor pollutants like NO and  $\text{NO}_2$  can result in serious human harm when their concentration exceeds certain exposure limits. Above regulatory limits, these gases increase the likelihood of cardiovascular, respiratory, and cancerous diseases. Gas sensors are therefore vital for detecting dangerous pollutant levels, so developing gas monitoring systems that can sensitively and selectively track these pollutants is a priority [23–26].

This study also focuses on the sensing behavior of  $\text{TiO}_2$  nanotube array sensors toward  $\text{NO}_2$  through a homemade gas-detection cell. The aim was to develop a sensitive  $\text{NO}_2$  sensor for low-concentration detection to assure the safety, health, and wellbeing of people by limiting the presence of  $\text{NO}_2$  in the air. The results of this study will help inform future research based on using  $\text{TiO}_2$  nanotubes for gas detection, as well as other potential applications. The synthesis process for the  $\text{TiO}_2$  nanotubes in this work is simpler and less costly than that of other methods like metal oxide elaboration. Thus, a gas sensor based on  $\text{TiO}_2$  nanotubes is more suitable for daily use.

## 2. Preparation of the Titania Nanotubes

To fabricate a  $\text{TiO}_2$  nanotube layer, we took a 1-mm-thick titanium metal sheet with 99.7% purity and subjected it to electrochemical anodization in an electrochemical unit. This process, as presented in Figure 1, is a relatively simple and efficient way to fabricate well-aligned and highly ordered  $\text{TiO}_2$  tubular structures. It involves two electrodes, a working electrode in titanium and the second counter electrode in platinum. The electrolyte solution in which the two electrodes are immersed is a mixture of 100 mL of ethylene glycol (EG), 1% ammonium fluoride ( $\text{NH}_4\text{F}$ ), and 2% ultrapure water, as presented in Figure 1.

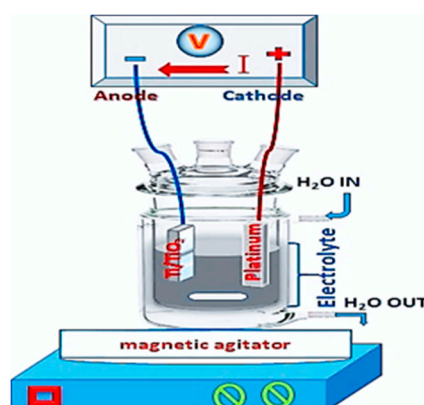


**Figure 1.** Schematic of anodization cell.

The  $\text{TiO}_2$  nanotubes are prepared in two steps, the first step involves polishing titanium at 120 V for 45 min., while the second step consists of preparing the  $\text{TiO}_2$  nanotubes at 60V for 15, 30, and 60 min. for the samples used in this study. Only porous structures were prepared on the sample surface at a lower anodization voltage, but when the anodization voltage was higher, the tubes started to form on the titanium metal surface. The applications of  $\text{TiO}_2$  nanotubes are closely related to their electrical, chemical, and optical properties. The obtained anodized  $\text{TiO}_2$  nanotubes are typically amorphous, and the conductivity of native  $\text{TiO}_2$  is very low, thus hampering applications

like gas sensing. In this study, we focused on modifying the  $\text{TiO}_2$  nanotubes to improve their electrical, chemical, and optical properties through thermal treatment. As such, the  $\text{TiO}_2$  nanotubes were annealed at  $400^\circ\text{C}$  for 3 hours in air to induce a phase transition from the amorphous structure to a crystalline anatase phase. X-ray diffraction scanning electron microscopy and transmission electron microscopy were then used to examine the nanotube array samples.

### 3. Characterization

Once the  $\text{TiO}_2$  nanotubes were prepared through anodization on metallic titania, we crystallized them through thermal annealing at  $400^\circ\text{C}$  for three hours in the air. The crystal structure of the produced  $\text{TiO}_2$  nanotubes was obtained through X-ray diffraction (XRD). The resulting crystal phases possessed better properties than amorphous  $\text{TiO}_2$ .

Claire modifications were observed on the  $\text{TiO}_2$  nanotubes before and after the heat treatment, as shown in Figure 2a,b. Definite XRD peaks at  $25.3^\circ$ ,  $37.7^\circ$ ,  $47.7^\circ$ ,  $53.8^\circ$ ,  $54.9^\circ$ ,  $62.5^\circ$ ,  $68.6^\circ$ ,  $70.5^\circ$ , and  $74.9^\circ$  can be seen in Figure 2, these correspond to the (101), (004), (200), (105), (211), (204), (116), (220), and (215) diffraction peaks of anatase  $\text{TiO}_2$  (JCPDS anatase card #21-1272), thus justifying the crystallization of the  $\text{TiO}_2$  layer through the formation of the anatase phase.

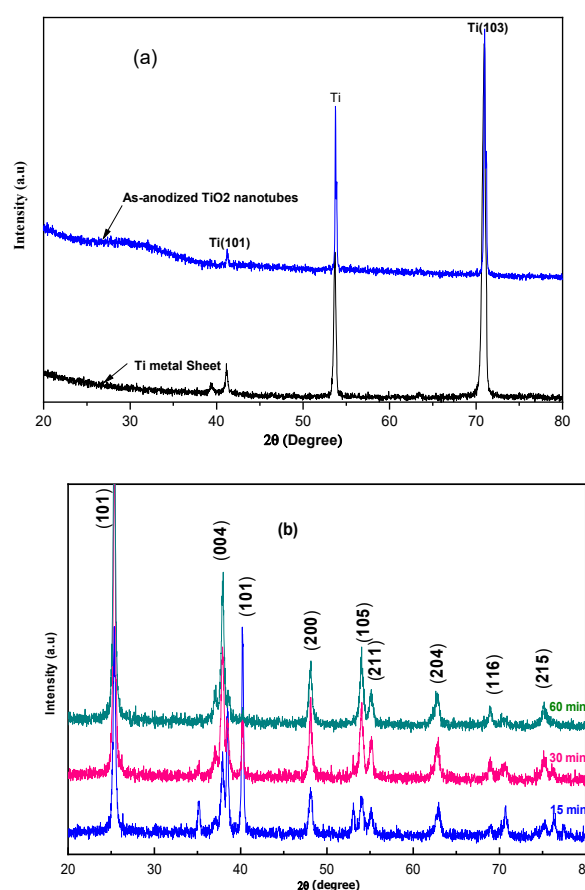


**Figure 2.** X-ray diffraction of (a) Ti metal sheet and as-anodized  $\text{TiO}_2$  nanotubes (b)  $\text{TiO}_2$  nanotubes formed at 15, 30 and 60 min and annealed at  $400^\circ\text{C}$  for 3 hours in air.

Figure 3 shows SEM images of the pure  $\text{TiO}_2$  nanotubes formed at 15, 30, and 60 min. and annealed at  $400^\circ\text{C}$  for 3 hours in air, and these show a highly ordered and organized nanostructure layer on the Ti substrate. Images of the cross-sectional SEM morphology indicate the elaboration of ordered and vertical titanium nanotubes, with the tube length varying at 3, 7, and  $9\ \mu\text{m}$  for 15, 30, and 60 min. anodization times, respectively. With a short anodization time, the nanotubes are short because the pore formation process has just started and the walls of the nanotubes are relatively thick. As the anodization time increases, the length of the nanotubes grows substantially. The electric field drives the oxidation of the metal at the bottom of the nanotube, while the electrolyte dissolves the



oxide at the top. This process allows for the vertical growth of the nanotubes and continued etching of the walls of the tubes, causing them to thin out and the pore diameter to widen. At extremely long anodization times, the tube length reaches a saturation point where growth stops or becomes negligible and leads to minimal changes in diameter compared to the growth in length.

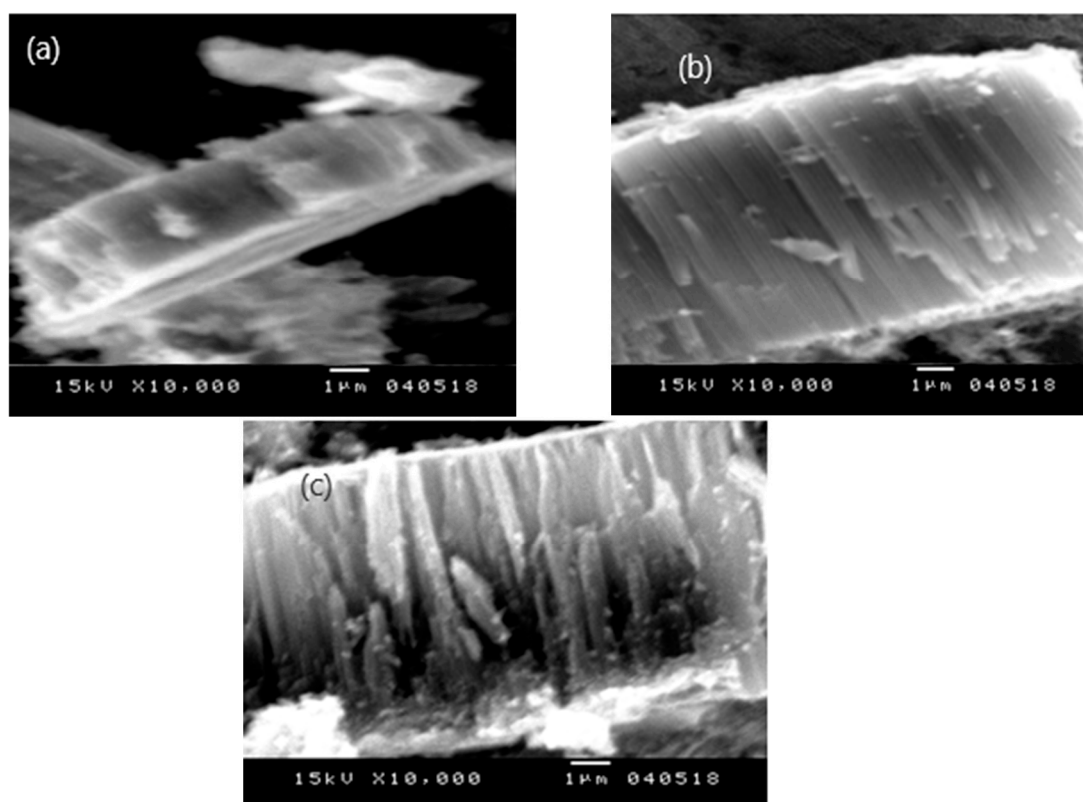


**Figure 3.** SEM cross-section of TiO<sub>2</sub> nanotubes formed at three different anodization times (a) 15, (b) 30, and (c) 60 min.

Transmission electron microscopy (TEM) was used to examine the morphology and uniformity of the TiO<sub>2</sub> nanotubes. Thus, a Philips CM30 transmission electron microscope was used to obtain accurate information about the morphology and size distribution of the pure TiO<sub>2</sub> nanotubes. Figure 4 shows the sample images obtained from the transmission electron microscope, thus confirming the nanomaterial structure of the TiO<sub>2</sub>. The TEM images (Figure 6) reveal that the followed methodology results in the fabrication and growth of highly ordered, structured nanotubes with an average inner diameter of about 100nm and a thickness in the nanotube walls of about 25nm.

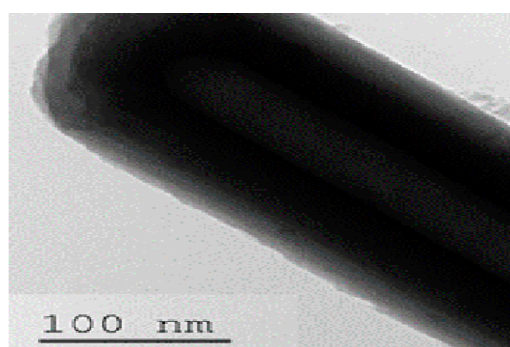


**Figure 4.** TEM image of TiO<sub>2</sub> nanotubes formed anodically at 60 min and annealed at 400 °C for 3 hours in air.

The impacts of the anodization time and nanotube length on the gas sensor's sensitivity are shown in Figure 5. From this, we can see that the shorter anodization cycles and shorter nanotube lengths result in enhanced sensitivity. For instance, a sensor with 3  $\mu\text{m}$  nanotubes anodized for 15 minutes exhibited a sensitivity of 99.62%. On the other hand, a sensor with a longer anodization time of 60 minutes had a sensitivity of only 24.12%. Thus, this study revealed that the length of a titanium nanotube is a crucial factor affecting the sensitivity of gas sensors in that shorter nanotubes are typically associated with improved sensitivity. In summary, the various characteristics of shorter titanium nanotubes—such as their increased surface area, low mass loading, and reduced diffusion path—contribute to their enhanced sensitivity and recovery potential.

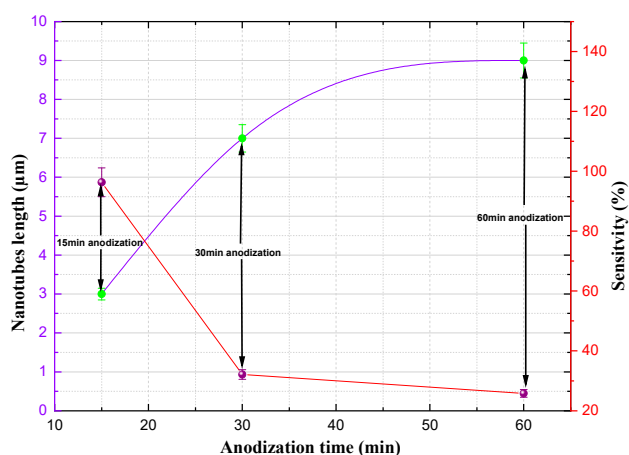


Figure 5. Nanotubes length and sensitivity as a function of anodization time.

#### 4. The Fabrication and Performance of the Sensing Device

After preparing the titanium dioxide nanotubes with the anodization method, their integration into an  $\text{NO}_2$  gas-sensing device was needed to ensure their effectiveness. For this purpose, front metal contacts were needed to measure electrical properties, so the choice and design of the front grid's contacts would affect the response of the final device in practical applications.

Figure 6 illustrates the design of the transducer on the  $\text{TiO}_2$  substrate with a tubular structure, and it shows the metallic electrodes evaporated on the front side of the nanotubular array substrate.

Additionally, a heater was integrated onto the back of the device in order to reach and maintain the desired operating temperature on the titania nanotubes' surface.

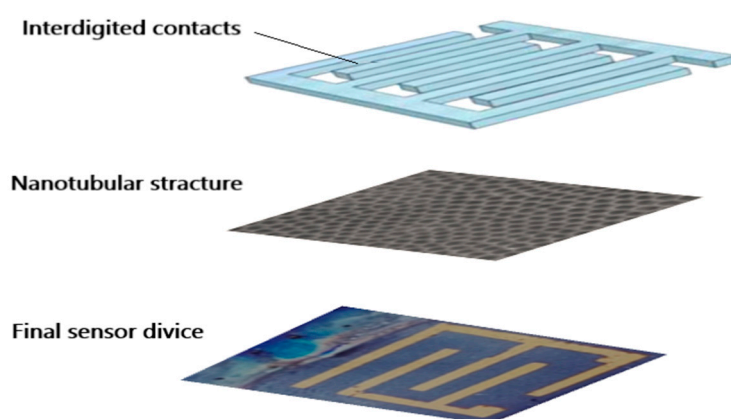


Figure 6. Design of a gas sensor device and  $\text{TiO}_2$  nanotubes array gas detector.

$\text{NO}_2$  and  $\text{TiO}_2$  nanotubes have numerous mechanisms that affect their electrical conductivity.  $\text{NO}_2$  can adsorb on a  $\text{TiO}_2$  surface through either physical or chemical means. The former is triggered by the Van der Waals effect, while the latter is achieved by the formation of bonds between the two.  $\text{NO}_2$  is a strong oxidant, meaning it readily grabs electrons from other substances. When  $\text{NO}_2$  comes into contact with a  $\text{TiO}_2$  surface, it snatches electrons away from the nanotube. This process is expressed in Equation (1):



At a low temperature, a reduction in conductivity is caused by the adsorption of  $\text{NO}_2$ . This phenomenon is accompanied by an increase in the transfer of electrons, but the elevated temperatures caused by the chemical reaction can speed up the process and increase the likelihood of  $\text{NO}_2$  molecules separating from the  $\text{TiO}_2$  nanotubes, thus reducing the impact of the  $\text{NO}_2$  on the nanotubes' conductivity.

Temperature can have a significant impact on how certain sensors function. In addition to the  $\text{NO}_2$  molecules' attachment and detachment, it can also influence the chemical reactions occurring on the nanotube surface.

To validate the response of a  $\text{TiO}_2$  nanotube device toward  $\text{NO}_2$  gas, a homemade gas-detection cell for  $\text{NO}_2$  gas sensing was made using the  $\text{TiO}_2$  nanotube material.

The optimization of the working temperature is illustrated in Figure 7, such that the experiment revealed that the sensor showed the best response at  $250^\circ\text{C}$ .

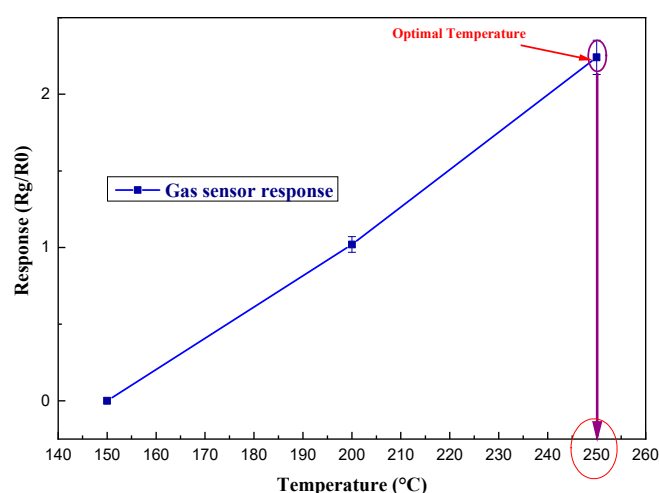


**Figure 7.** Optimization of the working temperature.

Nevertheless, to expand the applicability of titania nanostructures as gas sensors, several parameters need to be improved, namely the conductance of  $\text{TiO}_2$  in air, the sensing signal, the response, and the recovery times [27]. In this case, the dynamic response curve of the sample was measured in a range of 100 ppm. Figure 8 shows the gas-sensing measurements of  $\text{TiO}_2$  nanotubes within a 100 ppm  $\text{NO}_2$  gas atmosphere at  $250^\circ\text{C}$ .

The gas-sensing response ( $R$ ) is defined as the ratio of the resistance values of the sensor to the detected gas to the resistance in air, as follows:

$$R = \frac{R_g}{R_a} \quad (1)$$

Meanwhile, the gas sensitivity of the p-type sensor under  $\text{NO}_2$  oxidizing gas is calculated through the following equation, with more details being available in Refs. [28,29].

$$S (\%) = \frac{(R_g - R_a)}{R_a} * 100 \quad (2)$$

Where  $R_a$  represents the resistance of the film when exposed to air, and  $R_g$  denotes the resistance of the film when exposed to the analyte gas. The response time ( $\tau_r$ ) is the time for the resistor to change

from  $R_a$  to  $R_a+90\%(R_g-R_a)$ . Similarly, the recovery time ( $\tau_c$ ) is defined as the time required for the resistor to decrease from  $R_g$  to  $R_g-90\%(R_g-R_a)$ .

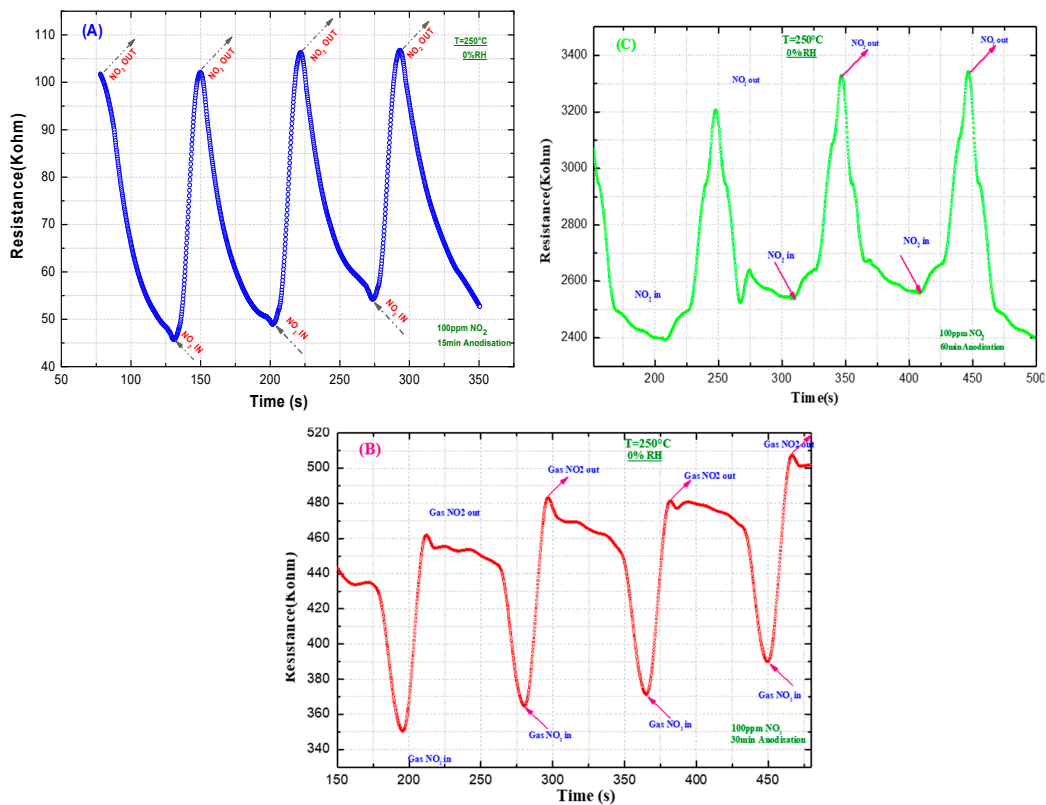


**Figure 8.** Sensor response characteristics and the dynamic response peak of TiO<sub>2</sub> nanotubes sensor against 100ppm NO<sub>2</sub> gas at 250°C for anodization times: (A) 15min, (B) 30min and (C) 60min.

The resistance response of TiO<sub>2</sub> nanotubes formed through 15, 30, and 60 min. of anodization were measured in 100 ppm NO<sub>2</sub> gas at a 250 °C working temperature. Good sensing performance was observed for the TiO<sub>2</sub> nanotubes anodized for 15 min, compared with anodized for 30 and 60 min., as indicated in Figure 8 and Table 1. In addition, the long-term stability of the TiO<sub>2</sub> sensor (anodized for 15 min) was verified, remaining stable for 40 cycles.

**Table 1.** The Sensing performance, response, and recovery times sensitivity and nanotube length of TiO<sub>2</sub> nanotubes operating at 15, 30, and 60min anodization for 100-ppm NO<sub>2</sub> gas concentration at 250°C working temperature.

Sensor-based TiO <sub>2</sub>	Response Time(s)	Recovery Time(s)	Sensitivity%
15 min Anodization	3.6±0.2	34±1.7	96.3±4.8
30 min Anodization	15.6±0.8	68.2±3.5	32.1±1.6
60 min Anodization	65±	132.8±6.6	25.8±1.3

The variation in the response of TiO<sub>2</sub> nanotubes at different anodization times for a 100 ppm NO<sub>2</sub> gas concentration is shown in Figure 9a. The NO<sub>2</sub> gas response was found to drop from 96% to 32% with an increase in anodization time from 15 to 30 min. before dropping further to 25.8% for a 60 min. anodization time. These lower response values are due to there being insufficient thermal energy to release the electrons from the trap defect levels and participate in the adsorption on the surface of the sensor film. In contrast, at an anodization time of 15 minutes, the maximum NO<sub>2</sub> gas response of 96% is obtained due to there being sufficient thermal energy to release the maximum number of electrons to overcome the trap levels below the conduction band and participate in the gas adsorption phenomenon. The response and



response-recovery times of TiO<sub>2</sub> nanotubes operating at different anodization times for a 100 ppm NO<sub>2</sub> gas concentration are summarized in Table 1 and Figure 9b. From these, it can be seen how both the response and recovery times increase with an increasing anodization time.

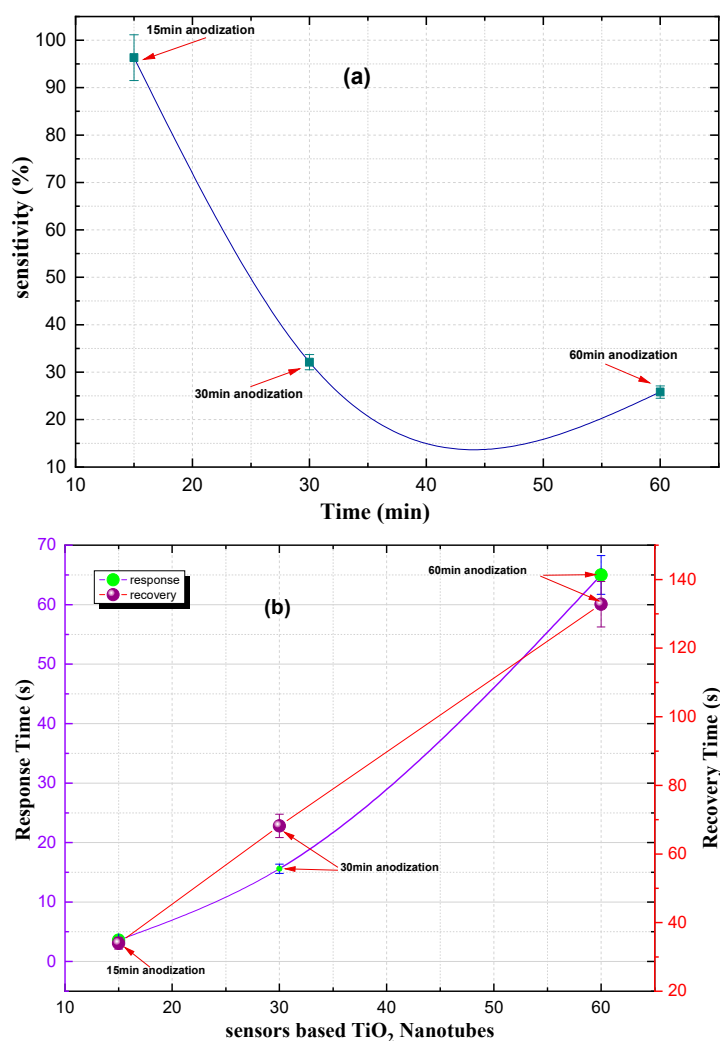


**Figure 9.** The Sensing performance (a) response, and (b) response-recovery times of TiO<sub>2</sub> nanotubes operating at 15, 30, and 60min anodization for 100 ppm NO<sub>2</sub> gas concentration at 250°C working temperature.

Figure 10 illustrates how the length of the titanium nanotubes affects the response time and recovery time of the gas sensor. It shows that sensors with shorter nanotubes have faster response and recovery times. For example, a sensor with 3-micrometer nanotubes has a response time of only 3.6 seconds, while a sensor with 9-micrometer nanotubes takes 65.5 seconds to respond. Additionally, the time it takes for the sensor to recover between measurements (i.e., the overlap time) also increases with nanotube length. These findings suggest that the length of the titanium nanotubes is a key factor in determining the overall performance of a gas detector.

Compared to long titanium nanotubes, they are therefore better suited for gas sensing. Investigations have also shown that doped and mixed titania structures are emerging as important materials for improving the conductometric properties of sensors [30–33].

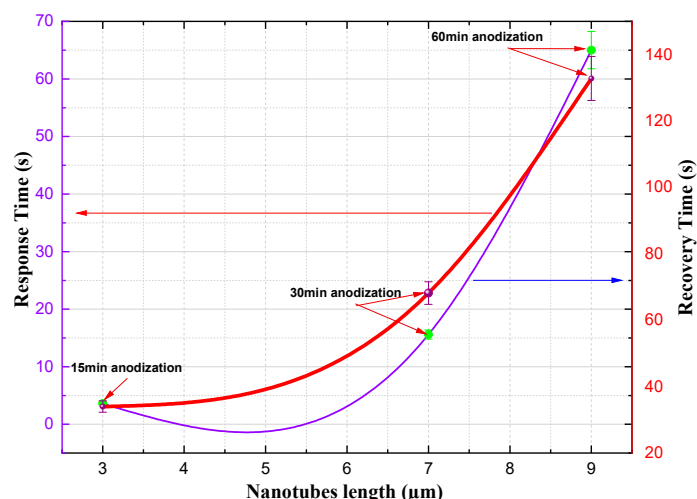


Figure 10. Response and recovery time as a function of nanotube length.

## 5. Conclusions

Titania nanotube arrays were synthesized in this study through a simple and relatively inexpensive electrochemical anodization method. XRD, SEM, and TEM characterizations demonstrated that this anodization process results in self-organized arrays of highly ordered vertical nanotubes on the Ti foil. Our research results also showed that the sensitivity of TiO<sub>2</sub> nanotubes for NO<sub>2</sub> gas detection is in the 24–99.6% range with a response time of 3.6 s at 250° C when exposed to a flow of around 100 ppm NO<sub>2</sub> gas. The preparation process is very simple and convenient, and the cost is relatively cheap. These advantages enhance the potential of TiO<sub>2</sub> nanotubes as excellent candidates for use in NO<sub>2</sub> gas detection. For instance, a sensor with 3-μm-long nanotubes after being anodized for 15 minutes exhibited a sensitivity of 99.62%.

To conclude, TiO<sub>2</sub> nanotubes exhibited high stability, good reproducibility, and high sensitivity for sensing NO<sub>2</sub>, thus positioning them as a promising material for NO<sub>2</sub>-sensing and other applications.

## References

- Öztürk, S.; Kılınc, N.; Öztürk, Z.Z. Fabrication of ZnO nanorods for NO<sub>2</sub> sensor applications: effect of dimensions and electrode position. *J. Alloys Compd.* 2013, 581, 196–201.
- Drmosh, Q. A.; Al Wajih, Y. A.; Al-Rammah, R.; Qamar, M.; Yamani, Z. H. Surface-engineered WO<sub>3</sub> thin films for efficient NO<sub>2</sub> sensing. *Applied Surface Science*. 2020, 517, 146235.
- Li, J.; Yang, M.; Guo, J.; Zhang, X.; Xu, Y.; Cheng, X.; Huo, L. Construction of highly efficient In<sub>2</sub>O<sub>3</sub>/SnO<sub>2</sub> sensor for real-time NO<sub>2</sub> monitoring at near room temperature. *Chemical Engineering Journal*. 2024, 498, 155286.
- Wu, Z.; Wang, Y.; Wu, Q.; Cheng, X.; Wang, Q.; Yang, Y.; Xie, E. SnO<sub>2</sub> grains with abundant surface oxygen vacancies for the Ultra-sensitive detection of NO<sub>2</sub> at low temperature. *Applied Surface Science* 2023, 614, 156223.
- Zhao, J.; Wang, H.; Cai, Y.; Zhao, J.; Gao, Z.; Song, Y. Y. The challenges and opportunities for TiO<sub>2</sub> nanostructures in gas sensing. *ACS sensors*. 2024, 9, 1644–1655.
- Ragab, A. H.; Al-Mhyawi, S. R.; Kamran, A. W.; Khan, I.; Khan, I. Highly selective sensing of toxic NO<sub>x</sub> gases for environmental monitoring using Ru-doped single walled TiO<sub>2</sub> nanotube: A density functional theory study. *Sensors and Actuators A: Physical*. 2024, 376, 115632.
- Asadpour, M.; Sadeghi, M.; Bani Asadi Bideski, A. An Ab-Initio Study on Mechanical Properties of Titanium Dioxide Single-Wall Nanotube. *Nano*. 2023, 18, 2350079.
- Fadlallah, M. M.; Eckern, U. Cation mono- and co-doped anatase TiO<sub>2</sub> nanotubes: an ab initio investigation of electronic and optical properties. *physica status solidi (b)*. 2023, 257, 1900217.
- Qamar, M.; Yoon, C.R.; Oh, H.J.; Lee, N.H.; Park, K.; Kim, D.H.; Kim, S.J. Preparation and photocatalytic activity of nanotubes obtained from titanium dioxide. *Catalysis Today*. 2008, 131, 3–14.
- Kim, J.H.; Zhu, K.; Kim, J.Y.; Frank, A.J. Tailoring oriented TiO<sub>2</sub> nanotube morphology for improved Li storage kinetics. *Electrochimica Acta*. 2013, 88, 123–128.

11. Ramanavicius, S.; Jagminas, A. Synthesis, Characterisation, and Applications of TiO and Other Black Titania Nanostructures Species (Review). *Crystals* 2024, 14, 647.
12. Kusior, A.; Radecka, M.; Zakrzewska, K.; Reszka, A.; Kowalski, B.J. Sensitization of TiO<sub>2</sub>/SnO<sub>2</sub> nanocomposites for gas detection. *Sensors and Actuators B: Chemical*. 2013, 189,251-259.
13. Gönüllü, Y.; Haidry, A.A.; Saruhan, B. Nanotubular Cr-doped TiO<sub>2</sub> for use as high-temperature NO<sub>2</sub> gas sensor. *Sensors and Actuators B: Chemical*. 2015, 217, 78-87.
14. Wu, J.; Zhang, C.; Li, Q.; Wu, L.; Jiang, D.; Xia, J. Application of TiO<sub>2</sub> to amperometric NO<sub>x</sub> sensors based on NASICON. *Solid State Ionics*. 2016, 292,32-37.
15. Shwetha, H.R.; Sharath, S.M.; Guruprasad, B.; Rudraswamy, S.B. MEMS based metal oxide semiconductor carbon dioxide gas sensor. *Micro and Nano Engineering*. 2022,16,100156.
16. Fernández-Ramos, M.D.; Capitán-Vallvey, L.F.; Pastrana-Martínez, L.M.; Morales-Torres, S.; Maldonado-Hódar, F.J. Chemoresistive NH<sub>3</sub> gas sensor at room temperature based on the carbon gel-TiO<sub>2</sub> nanocomposites. *Sensors and Actuators B: Chemical*. 2022,368,132103.
17. Ma, S.; Jia, J.; Tian, Y.; Cao, L.; Shi, S.; Li, X.; Wang, X. Improved H<sub>2</sub>S sensing properties of Ag/TiO<sub>2</sub> nanofibers. *Ceramics International*. 2016, 42, 2041-2044.
18. Wang, X.; Li, S.; Xie, L.; Li, X.; Lin, D.; Zhu, Z. Low-temperature and highly sensitivity H<sub>2</sub>S gas sensor based on ZnO/CuO composite derived from bimetal metal-organic frameworks. *Ceramics International*. 2020, 46,15858-15866.
19. Arruda, L.B.;Santos, C.M.; Orland, M.O.; Schreiner, W.H.; Lisboa-Filho, P.N. Formation and evolution of TiO<sub>2</sub> nanotubes in alkaline synthesis. *Ceramics International*. 2015, 41,2884-2891.
20. Batool, S.A.; Salman, M.M.; Javed, M.A.; Niaz, A.; Rehman, M.A.U. A review on the fabrication and characterization of titania nanotubes obtained via electrochemical anodization. *Surfaces*. 2022, 5,456-480.
21. Hailiang, L.; Wang, G.; Niu, J. et al. Preparation of TiO<sub>2</sub> Nanotube arrays with efficient photocatalytic performance and super hydrophilic properties utilizing anodized voltage method. *Results Phys*. 2019, 14,0102499.
22. Galstyan, V.; Macak, J.M.; Djenizian, T. Anodic TiO<sub>2</sub> nanotubes: a promising material for energy conversion and storage. *Appl Mater Today*. 2022, 29,101613.
23. Wang, C.; Yin, L.; Zhang, L.; Xiang, D.; Gao, R. Metal oxide gas sensors: sensitivity and influencing factors. *Sensors*. 2010,10,2088-2106.
24. Arenas-Hernandez, A.; Zúñiga-Islas, C.; Mendoza-Cervantes, J.C. A study of the effect of morphology on the optical and electrical properties of TiO<sub>2</sub> nanotubes for gas sensing applications. *The European Physical Journal Applied Physics*. 2020,90,30102.
25. Tian, X.; Cui, X.; Lai, T.; Ren, J.; Yang, Z.; Xiao, M.; Wang, Y. Gas sensors based on TiO<sub>2</sub> nanostructured materials for the detection of hazardous gases: A review. *Nano Materials Science*. 2021,3,390-403.
26. Kim, W. T.; Kim, I. H.; Choi, W. Y. Fabrication of TiO<sub>2</sub> nanotube arrays and their application to a gas sensor. *Journal of nanoscience and nanotechnology*. 2021,15, 8161-8165.
27. Ragab, A.H.; Al-Mhyawi, S.R.; Kamran, A.W.; Khan, I.; Khan, I. Highly selective sensing of toxic NO<sub>x</sub> gases for environmental monitoring using Ru-doped single walled TiO<sub>2</sub> nanotube: A density functional theory study. *Sensors and Actuators A: Physical*. 2024,376,115632.
28. Tian, X.; Cui, X.; Lai, T.; Ren, J.; Yang, Z.; Xiao, M.; Wang, Y. Gas sensors based on TiO<sub>2</sub> nanostructured materials for the detection of hazardous gases: A review. *Nano Materials Science*.2021, 3, 390-403.
29. Deshmukh, S.B.; Bari, R.H. Nanostructured ZrO<sub>2</sub> thin films deposited by spray pyrolysis techniques for ammonia gas sensing application. *International Letters of Chemistry, Physics and Astronomy*. 2015,56,120-130.
30. Hyodo, T.; Okusa, T.; Sakata, W.; Ueda, T.; Shimizu, Y. Impacts of Surface Modification of Pt-Sensing Electrodes with Au on Hydrogen-Sensing Properties and Mechanism of Diode-Type Gas Sensors Based on Anodized Titania. *ACS sensors*. 2022,8,61-70.
31. Yu, W.; Chen, D.; Li, J.; Zhang, Z. TiO<sub>2</sub>-SnS<sub>2</sub> Nanoheterostructures for High-Performance Humidity Sensor. *Crystals* 2023, 13, 482.

32. Tong, X.; Shen, W.; Zhang, X.; Corriou, J.P.; Xi, H. Synthesis and density functional theory study of free-standing Fe-doped TiO<sub>2</sub> nanotube array film for H<sub>2</sub>S gas sensing properties at low temperature. *Journal of Alloys and Compounds*. 2020,832,155015.
33. Zavatski, S.; Neilande, E.; Bandarenka, H.; Popov, A.; Piskunov, S.; Bocharov, D. Density functional theory for doped TiO<sub>2</sub>: Current research strategies and advancements. *Nanotechnology*. 2024,35, 192001.

**Disclaimer/Publisher's Note:** The statements, opinions and data contained in all publications are solely those of the individual author(s) and contributor(s) and not of MDPI and/or the editor(s). MDPI and/or the editor(s) disclaim responsibility for any injury to people or property resulting from any ideas, methods, instructions or products referred to in the content.